Directional control of cell motility through focal adhesion positioning and spatial control of Rac activation

Nan Xia,* Charles K. Thodeti,* Tom P. Hunt,† Qiaobing Xu,‡ Madelyn Ho,* George M. Whitesides,‡ Robert Westervelt,† and Donald E. Ingber*,[1]

*Vascular Biology Program, Departments of Pathology and Surgery, Children's Hospital and Harvard Medical School; †Department of Physics and Division of Engineering and Applied Sciences; and ‡Department of Chemistry and Chemical Biology, Harvard University, Boston, Massachusetts, USA

ABSTRACT **Local physical interactions between cells and extracellular matrix (ECM) influence directional cell motility that is critical for tissue development, wound repair, and cancer metastasis. Here we test the possibility that the precise spatial positioning of focal adhesions governs the direction in which cells spread and move. NIH 3T3 cells were cultured on circular or linear ECM islands, which were created using a microcontact printing technique and were 1 μm wide and of various lengths (1 to 8 μm) and separated by 1 to 4.5 μm wide nonadhesive barrier regions. Cells could be driven proactively to spread and move in particular directions by altering either the interisland spacing or the shape of similar-sized ECM islands. Immunofluorescence microscopy confirmed that focal adhesions assembled preferentially above the ECM islands, with the greatest staining intensity being observed at adhesion sites along the cell periphery. Rac-FRET analysis of living cells revealed that Rac became activated within 2 min after peripheral membrane extensions adhered to new ECM islands, and this activation wave propagated outward in an oriented manner as the cells spread from island to island. A computational model, which incorporates that cells preferentially protrude membrane processes from regions near newly formed focal adhesion contacts, could predict with high accuracy the effects of six different arrangements of micropatterned ECM islands on directional cell spreading. Taken together, these results suggest that physical properties of the ECM may influence directional cell movement by dictating where cells will form new focal adhesions and activate Rac and, hence, govern where new membrane protrusions will form.—Xia, N., Thodeti, C. K., Hunt, T. P., Xu, Q., Ho, M., Whitesides, G. M., Westervelt, R., Ingber, D. E. Directional control of cell motility through focal adhesion positioning and spatial control of Rac activation. *FASEB J.* 22, 1649–1659 (2008)**

Key Words: migration · extracellular matrix · microcontact printing · cytoskeleton · mechanical · traction

DIRECTIONAL CELL MOTILITY IS CRITICAL for normal tissue development as well as the immune response, angiogenesis, and cancer metastasis. Most work on directional control of cell movement has focused on gradients of soluble chemokines (1) that, in turn, generate intracellular gradients of signal transduction (1–4). However, cell movement also can be influenced by physical interactions between cells and their extracellular matrix (ECM) adhesions. For example, cells move from regions of high ECM compliance to more stiff regions, a process as known as durotaxis (5–7). When plated on single-cell sized ECM islands of different geometric shapes created with microfabrication techniques, various cells preferentially extend new motile processes (*e.g.*, lamellipodia, filopodia, microspikes) from their corners rather than along their edges (8, 9). Cell migration direction also can be controlled by constraining cell geometry using similar microengineered ECM islands and then releasing the physical restrictions to movement using electrochemical techniques (10). Importantly, these findings are relevant because cells also preferentially extend and migrate along ECMs with specialized shapes (*e.g.*, fibrils) during tissue development (11) and tumor angiogenesis (12). However, the mechanism by which physical interactions between cells and ECM govern the direction in which they move remains unclear.

The effects of ECM on directed cell migration are mediated by transmembrane integrin receptors that mechanically couple to submembranous focal adhesion proteins, such as vinculin, that physically link the ECM to the intracellular cytoskeleton (1, 13). Integrin binding influences cell movement by stimulating the small GTPase Rac (14–16), which activates the Arp2/3 complex (17) and thereby nucleates actin polymerization (18–20), which drives lamellipodial protrusion (21, 22). Arp 2/3 also transiently associates with vinculin and colocalizes with it in nascent focal adhesions known as focal complexes (23). Interestingly, activated Rac fails to promote lamellipodia extension in vinculin

[1] Correspondence: Vascular Biology Program, KFRL 11.127, Children's Hospital, Boston, MA 02115, USA. E-mail: donald.ingber@childrens.harvard.edu

doi: 10.1096/fj.07-090571

null cells (24), suggesting that focal adhesion assembly may play an important role in directional cell motility. This possibility is supported by the observation that single cells anchored to polygonal ECM islands preferentially form focal adhesions in their corners near sites where new lamellipodia will form when the cells are stimulated with soluble chemokines, and cells on circular islands (*i.e.*, without corners) do not exhibit any directional bias (9). Focal adhesions also appear to form preferentially, directly behind the leading edge of cells migrating in the direction of increasing ECM stiffness (25, 26), and changes in mechanical force transfer across integrins can modulate focal adhesion assembly (27). Taken together, these findings imply that the spatial positioning of focal adhesions may determine the location in which new motile processes form, and hence, govern the direction in which cells move.

If these findings are true, then it should be possible to proactively dictate the direction in which cells will move by controlling the location where cells can form new focal adhesions. In the present study, we test this hypothesis directly by using microcontact printing methods to create culture substrates containing ECM islands on the size scale of individual focal adhesions surrounded by nonadhesive regions, and then determining whether altering island shape or position influences the direction of cell spreading and movement.

MATERIALS AND METHODS

Experimental system

The micropatterned substrates containing micrometer-sized ECM islands separated by nonadhesive barrier areas were created using microcontact printing and coated with rhodamine conjugated fibronectin (Cytoskeleton, Denver, CO, USA), as described (28, 29). Mouse NIH 3T3 fibroblasts were maintained at 37°C under 10% CO_2 in high-glucose Dulbecco's modified Eagle's medium (DMEM), supplemented with 10% fetal bovine serum, glutamine (0.3 mg/mL), penicillin (100 U/ml), streptomycin (100 μg/mL), and 20 mM HEPES. Subconfluent cell monolayers were serum-starved for 1 day, trypsinized, and plated on micropatterned substrates in DMEM containing high-density lipoprotein (10 μg/mL), transferrin (5 μg/mL), and 1% bovine serum albumin. The plating density was low to minimize cell-cell contacts.

Reagents

Mouse antivinculin antibody, fluorophore-conjugated secondary antibodies, fluoresceinated phalloidin, ML-7 and FITC-labeled-poly-L-lysine were purchased from Sigma (St. Louis, MO, USA). The motility factor, human PDGF-BB was purchased from BioVision (Mountain View, CA, USA). The FRET probe, Raichu-Rac1, was kindly provided by Dr. Michiyuki Matsuda (Osaka University, Osaka, Japan) (30).

Microscopy and imaging

We used a serum-free cell culture medium for live cell imaging, as described previously (8). Live cell images were recorded with a CCD camera (Hamamatsu, Tokyo, Japan) on a Diaphot 300 inverted microscope (Nikon, Tokyo, Japan) equipped with phase contrast optics and epifluorescence illumination and processed using the computerized image acquisition and analysis tools of IP Lab Spectrum and RatioPlus software (Scanalytics, Fairfax, VA, USA). The microscope was also equipped with an on-stage heater that maintained the temperature at 37°C at all times, and the culture medium was covered with a thin layer of mineral oil to prevent evaporation. Immunofluorescence microscopy was performed as described (8). Fluorescence images were acquired on a Leica TCS SP2 confocal laser scanning microscope with an ×63/1.4 NA oil immersion objective (Leica Microsystems, Bannockburn, IL, USA) and processed using Leica software or Adobe Photoshop (Adobe Systems, San Jose, CA, USA). Morphometric analysis of cell shape, orientation, and migration was performed by outlining the borders of individual cells within differential interference contrast images using the computerized image acquisition and analysis tools described above; 25 to 50 cells were analyzed for each experimental condition. Cell elongation was defined as the ratio of the maximal to minimal cell length. In the migration assays, cells were stimulated with PDGF (50 ng/ml), and the centroids of the migrating cell recorded at 20 min intervals over 8 h were plotted and connected to generate the migration path, which was then used to calculate the speed and direction of cell migration.

Rac FRET analysis

NIH 3T3 cells were transfected with the FRET reporter of Rac activity, Raichu-Rac1 (30), using effectene transfection reagent (Qiagen, Valencia, CA, USA) and cultured for 24 h on the different micropatterned substrates in serum-free medium. We studied cells cultured on the 3L-4.5,1 pattern in studies analyzing spatial control of Rac activation dynamics at high resolution because this pattern has the largest difference in island spacing between the *x* and *y* directions, which greatly increases our ability to perform this difficult visualization technique. For FRET analysis, fluorescence images were acquired every minute on a Leica TCS SP2 confocal laser-scanning microscope with an ×63/1.4 NA oil immersion objective using Leica FRET sensitization software (CFP and FRET excitation at 458 nm; YFP excitation at 514 nm). Calibration images were acquired from the samples containing only Donor (CFP), Acceptor (YFP), and FRET (Raichu-Rac1), respectively, and the apparent FRET efficiency was automatically calculated by the software. We also validated the efficiency of the Raichu-Rac1 construct by acceptor photobleaching method, which confirmed that donor (CFP) fluorescence and associated FRET increases when the acceptor (YFP) is bleached.

Computational modeling

In the computer simulation program that was performed using MATLAB, "cells" represented by *N* circles with a spherical diameter *D* were generated at random locations above a microarray of discrete "virtual" ECM islands separated by nonadhesive regions. The initial contact area between the adhering cell and the substrate was assumed to be circular with a diameter of *D′*; both *D* and *D′* were set at 15 μm. Every point (point resolution was set at 0.5 μm) along the cell's boundary where it contacted an ECM island had an equal opportunity to extend membrane protrusions in a circular sweep outside of the cell body with a radius *r*. The size distribution of radius *r* of new membrane extensions was set so that large extensions decreased exponentially with *r* based

on experimental observations of living cells. Any protrusion that contacted a neighboring ECM island formed a new focal adhesion and remained anchored; other protrusions retracted back onto the cell. The cell boundary was then modified to incorporate the newly formed adhesive contacts to form a new polygonal map of the extended cell border as it spread over the cell-substrate interface. This completed one cycle of simulated cell spreading, and then the process was reiterated multiple times.

RESULTS

Control of cell spreading by varying ECM island shape and position

Six different planar microarrays of focal adhesion-sized circular or linear FN islands, separated by nonadhesive regions, were created using microcontact printing. As displayed in **Fig. 1**, these included patterns of 1 μm diameter circular FN islands that were either separated by 3 μm in both the *x* and *y* directions (1C-3,3) or by 1.5 μm in the *x* direction and 3 μm in the *y* direction (1C-1.5,3); linear FN islands 1 μm high (*y* direction) and 3 or 8 μm wide (*x* direction) separated by 3 μm in both directions (3L-3,3 and 8L-3,3 respectively); linear FN islands 3 μm wide × 1 μm high separated by 4.5 and 1 μm in *x* and *y* directions, respectively (3L-4.5,1); and linear 8 μm wide × 1 μm high FN lines equally spaced by 3 μm in both directions, but staggered along a 60° offset (8L-3,3st).

When NIH 3T3 cells were plated on these substrates in serum-free medium, cell spreading proceeded in a manner different from that on standard FN-coated plastic substrates. For example, cell spreading reached maximal levels within ~30 min after plating on control FN-coated dishes, and only after this time did the cells begin to elongate in an anisotropic manner and exhibit a bipolar form (**Fig. 2** left). In contrast, when cells were cultured on the isotropic microarray of 1 μm FN circles

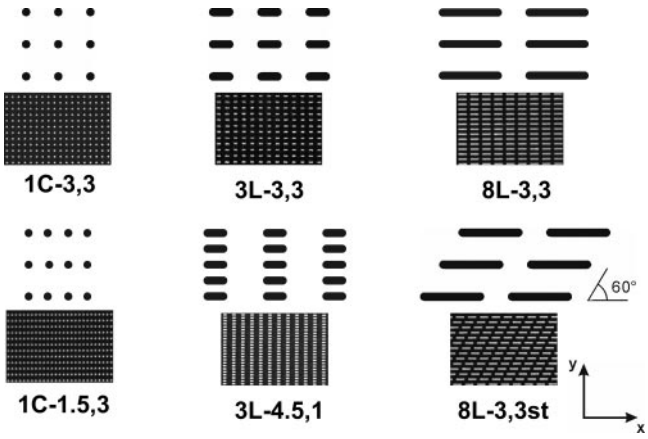

Figure 1. Schematic designs of a small region from six different planar microarrays of FN islands used in this study, and fluorescence micrographs showing corresponding substrates created with the microcontact printing technique that were imprinted with fluorescent fibronectin.

(1C-3,3) they spread more slowly and to a lesser degree over the first 2 h after plating (Fig. 2, middle). Although directional extension initiated about the same time, the cells on the 1C-3,3 micropattern also elongated more gradually and to a lesser degree than control cells on the unpatterned substrates. In contrast, when cells were cultured on similarly shaped FN islands that were more closely spaced in the *x* direction (1C-1.5,3), cell spreading and directional elongation initiated more rapidly and increased in parallel during the same time course (Fig. 2, right). We have previously shown that cells can attach and spread on these microfabricated substrates (31) as well as standard ECM-coated substrates (32) in the absence of *de novo* protein synthesis, and we observed similar differences in spreading rates when protein synthesis was inhibited using cycloheximide (data not shown). Comparison of cells on all six different FN island arrangements revealed that the isotropic arrangement of FN circles (1C-3,3) and the anisotropic array of linear islands with the smallest interisland spacing (3L-4.5,1) produced the lowest and greatest cell elongation, respectively, when analyzed at 50 min, 2 h or 8 h after cell plating (**Fig. 3*A***). However, virtually all of the linear substrates and the anisotropic array of circular FN islands exhibited a similar high level of elongation after 8 h of culture. Interestingly, differences in cell elongation could not be detected until 2 h after plating, and they became significant ($P<0.05$) only after 8 h (Fig. 3*A*).

Analysis of elongated cells on the different micropatterned substrates at similar times confirmed that, although cells did not display a preferred orientation on the isotropic array of FN circles (1C-3,3), cells on the anisotropic array of similar shaped FN islands (1C-1.5,3) elongated in a highly oriented manner (Fig. 3*B*). In our analysis, we determined the average angular orientation of cells by measuring the direction of their longest axis over a range from 0 to 90°, and, thus, randomly oriented cells will display an average orientation of 45° with a very wide distribution of values, and this was what we observed for cells on the 1C-3,3 pattern (Supplemental Fig. S1). The cells also spread and aligned preferentially along the main axis of the linear FN islands even when they were distributed isotropically (3L-3,3 and 8L-3,3) or in a staggered pattern (8L-3,3st), and greater cell alignment was observed on the longer islands (Fig. 3*B*). Decreasing the spacing between FN circles to 1.5 μm in the *x* direction (1C-1.5,3) similarly promoted greater cell orientation in this direction, and decreasing the spacing between linear islands in the *y* direction to 1 μm while simultaneously increasing the interisland separation in the *x* direction to 4.5 μm (3L-4.5,1) produced the most potent effect causing almost all of the cells to orient in the *y* direction (90°) (Fig. 3*B*).

The efficiency of cell alignment also correlated with the degree of alignment of F-actin filament bundles in the cytoskeleton within cells on these various substrates (Fig. 3*C*). Moreover, when we examined cells cultured on FN island microarrays, bright vinculin staining

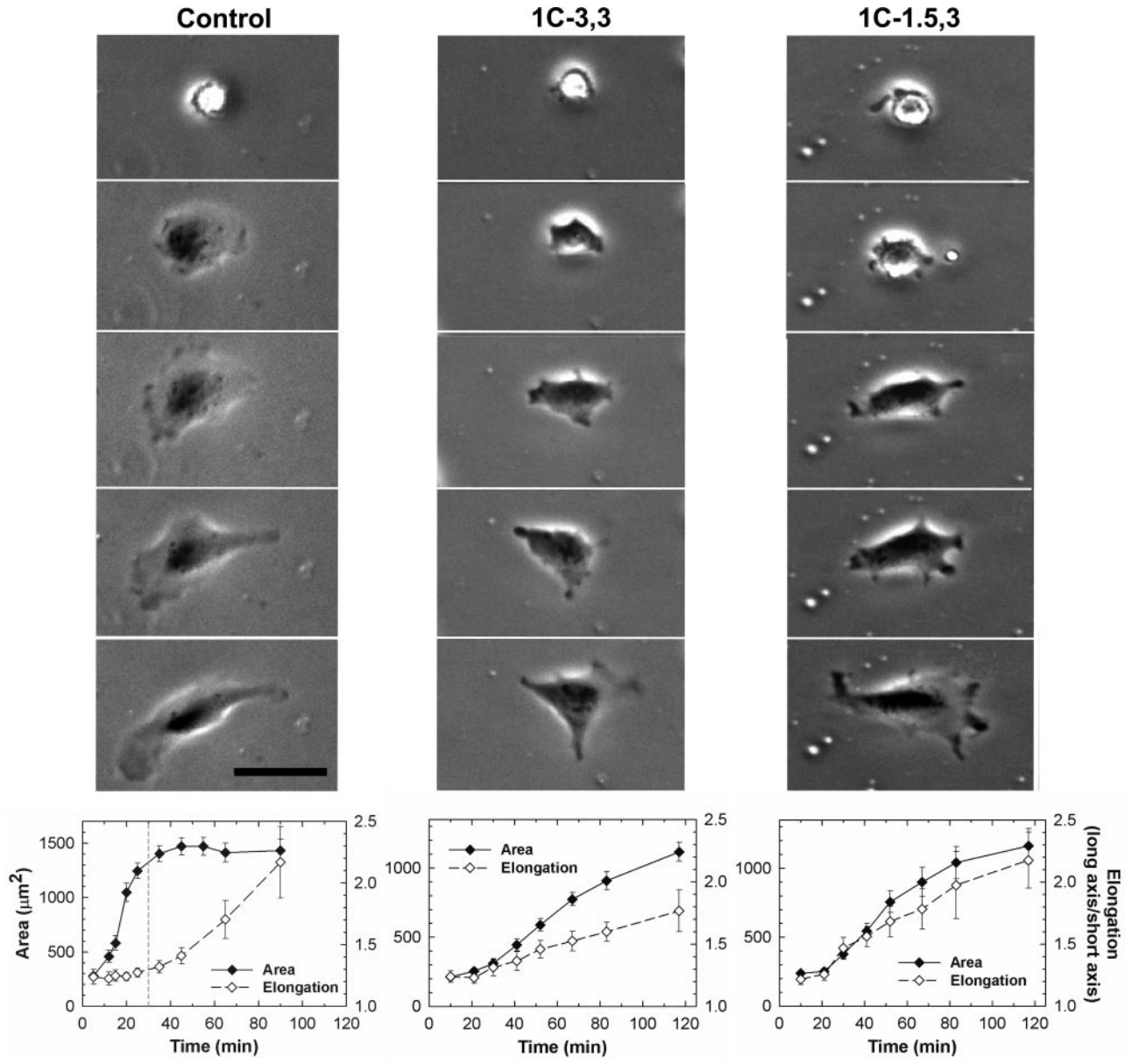

Figure 2. Effects on the dynamics of cell spreading. Top: time-lapse phase contrast microscopic images recorded at 5, 20, 40, 60, and 80 min (top to bottom) after plating on standard FN-coated plastic (left) *vs.* micropatterned substrates with two different patterns: 1C-3,3 (middle) and 1C-1.5,3 (right). Bottom: graphs showing the effects of the respective substrates on projected cell area and elongation during the progress of spreading. Scale bar = 40 μm.

could be detected in regular shapes and patterns that corresponded directly to the form and position of each microfabricated FN island (**Fig. 4**), as observed in previous studies (28, 38). Interestingly, in contrast to effects on elongation that were only observed after 8 h, significant micropattern-dependent differences in cell alignment were detected within 50 min after plating (Fig. 3*B*). Thus, the position of these focal adhesion-sized islands influenced cell orientation from the earliest times after cell adhesion, and once alignment was established it appeared to govern the direction in which cells would preferentially reorient their actin cytoskeleton and elongate their shape at later times. In contrast, when these same adhesive islands were coated with polylysine rather than FN, the effects of these substrates on cell orientation and elongation were greatly reduced (Fig. 3*A*, *B*), indicating that specific binding interactions between cells and ECM are critical for these observed directional responses.

Initial cell orientation and elongation govern the direction of cell movement

We next examined whether the effects of ECM island shape and distribution on cell orientation and elongation that we observed at early times influence the direction of cell motility when stimulated by soluble chemokines. When the motility factor, PDGF, was added to the cells that had spread for 3 h in the

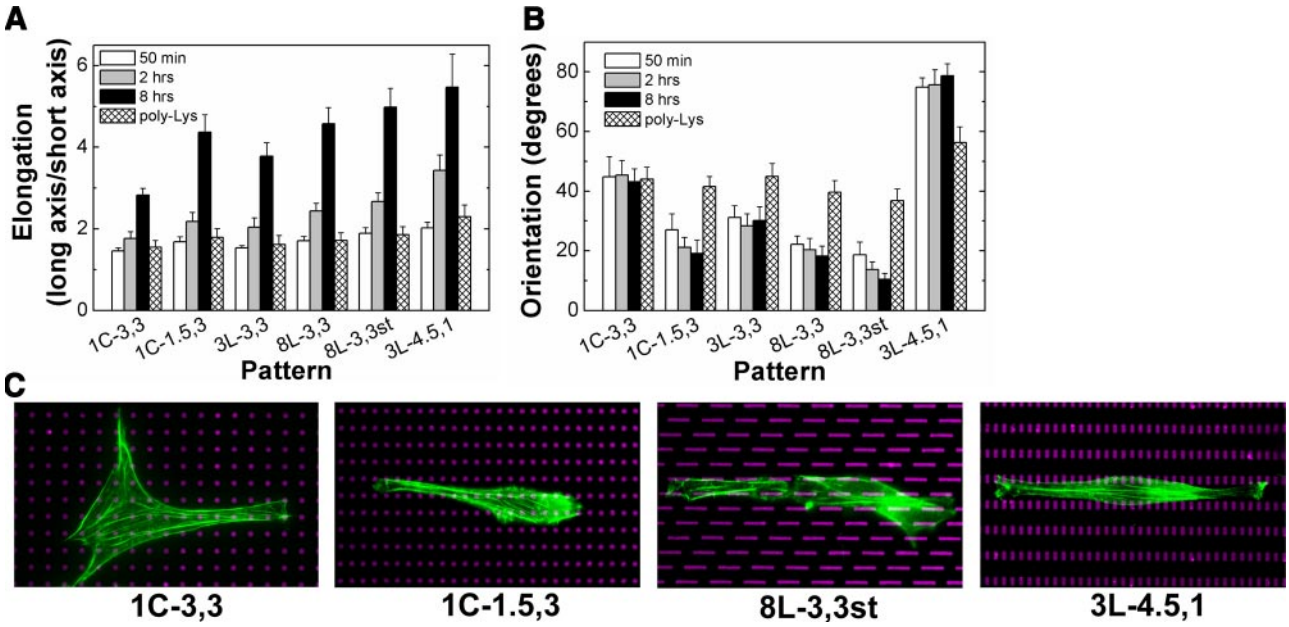

Figure 3. Effects of different FN microarrays on cell elongation, orientation, and cytoskeletal organization. *A*) Cell elongation (ratio of the longest axis of the cell to its shortest) is presented for cells cultured for 50 min (white bars), 2 h (gray bars), or 8 h (black bars) on different micropatterned FN substrates labeled as indicated in Fig. 1, or for 6 h on similar island microarrays coated with polylysine (cross-hatched bars). *B*) Cell orientation (degrees of the longest axis deflected from horizontal) measured under similar conditions and at the same times as in *A*. *C*) Overlay of fluorescence micrographs showing the arrays of representative FN microisland patterns (magenta) and the actin cytoskeleton (green) of adherent cells cultured for 8 h.

serum-free medium, cell migration speeds were similar on all six micropatterned substrates; however, the direction of movement differed significantly (**Fig. 5*A***). Again, cell migration direction was essentially random (45° with a wide distribution) on the isotropic FN circles and more oriented on the anisotropic patterns and linear FN islands (Fig. 5*A*). But most importantly, the direction of motility and the efficiency of orientation scaled directly with the effects of these same micropatterned substrates on cell orientation at earlier times (Figs. 3*B vs.* 5*A*). For example, whereas cells migrated in a random Brownian walk on the isotropic array of FN circles (Fig. 5*B*), cells could be made to preferentially migrate in either the *x* or *y* direction with great efficiency by decreasing interisland spacing in the *x* or *y* direction using the 1C-1.5,3 and 3L-4.5,1 substrates, respectively (Fig. 5*B*). Thus, the early effects of FN island shape and position on cell orientation govern both the orientation in which cells will elongate and the direction in which they will move when stimulated with soluble motility factors.

Cells protrude new membrane processes near nascent focal adhesions

Protrusion of new membrane processes, such as lamellipodia and filopodia, is fundamental to cell spreading and migration (37). We, therefore, monitored formation of new lamellipodia during cell spreading on the micropatterned substrates. During this process, cells appeared to preferentially form new membrane protrusions near regions close to the micropatterned FN

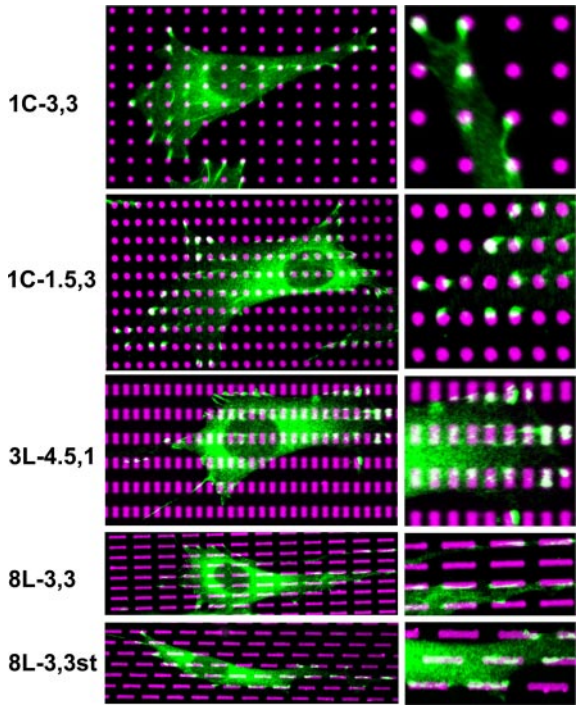

Figure 4. The shape and distribution of vinculin-containing focal adhesions corresponds to those of the micropatterned FN islands. Immunofluorescence microscopic overlay images of cells cultured for 8 h on different micropatterned distributions (indicated at left) of rhodamine-FN-coated islands (magenta) and stained with antivinculin antibodies (green). Insets: higher magnification views of the codistribution of vinculin and rhodamine FN (white) within the corresponding images at left.

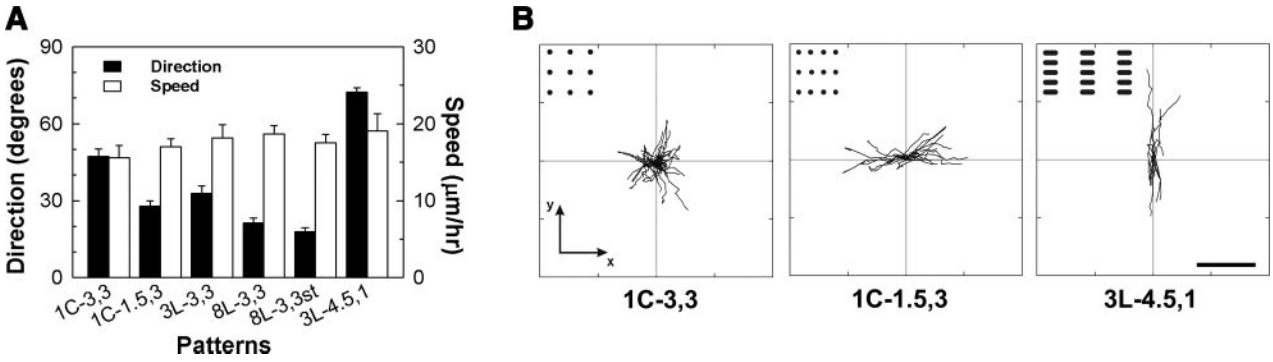

Figure 5. Control of cell migration by altering the shape, size, and position of FN adhesive islands. *A*) Graph showing the effects of the various FN microarrays on cell migration speed (white bars; μm/h) and direction (black bars; degrees deflected from horizontal) in NIH3T3 cells stimulated with PDGF (50 ng/ml). *B*) Representative examples of migration paths of the PDGF-stimulated cells migrating on three different FN microarray patterns: 1C-3,3 (left), 1C-1.5,3 (middle) and 3L-4.5,3 (right). The position of cell centroids was measured over 8 h at 20 min intervals. Scale bar=100 μm.

islands and to extend these processes over both adjacent FN-coated islands and nearby nonadhesive areas (**Fig. 6**). These small lamellipodial protrusions that extend over nonadhesive regions during early phases of cell spreading are actin-rich, as previously demonstrated (9), and confirmed by fluorescent phalloidin staining (data not shown). Analysis of 60 protrusions within randomly chosen cells spreading on all six micropatterned substrates revealed that ~88% of protrusions originated from regions of the cell directly above or adjacent to FN islands along the cell periphery. Dynamic microscopic analysis of living cells revealed that these extending processes stabilized when the protrusions contacted adjacent FN islands and formed new cell-ECM adhesions, whereas those that extended over nonadhesive regions of the substrate retracted back onto the cell surface. Adhesion of the new processes to the nearby FN islands also was accompanied by an overall change of cell shape as the cell body was progressively pulled forward to cover the newly occupied adhesive area.

Spatial control of Rac activation

The small GTPase, Rac1 controls lamellipodia formation, and it can be activated by cell-ECM adhesion in an integrin-dependent manner (14–16). Analysis of the spatial distribution of Rac activity in cells cultured on the different FN microarrays (**Figs. 7** and **8**) using an intramolecular Rac1-FRET reporter (30) revealed higher FRET efficiency (and hence Rac GTPase activation) in regions directly above FN islands compared with the intervening nonadhesive areas beneath a cell (Fig. 7*A*). Quantification of the results of FRET analysis of multiple cells grown on pattern 3L-3,3 demonstrated that Rac activation levels were ~3× higher in regions overlying FN islands than in the nonadhesive areas beneath spreading cells, and >6× higher than that observed in regions of the substrate that were not covered by cell membrane (Fig. 7*B*).

Because these cells were cultured in serum-free medium without added chemokines, the Rac activity we observed was likely primarily due to signaling elicited in response to new integrin binding to these micropatterned FN islands. This point was made even clearer when we monitored dynamic changes of Rac activity as cells progressively spread across multiple FN islands of pattern 3L-4.5,1. Lamellipodia extended centripetally from existing focal adhesions near the cell periphery and transiently crossed over adjacent nonadhesive areas to contact adjacent FN islands (Fig. 8). When the same cell was followed over a period of 15 min, the cell could be observed to pull its body forward to cover the newly contacted FN island and then to extend another new process in the same direction from this nascent adhesion site; reiteration of this process resulted in progressive spreading and movement of the cell in a consistent direction, as dictated by the smaller interisland spacing in the one direction relative to the other in the micropattern (3L-4.5,1) used in this study (Fig. 8*A*). Importantly, the Rac-FRET analysis revealed that Rac1 became locally activated within 2–3 min after the cell's surface membrane contacted each new FN island, and this process of Rac activation reiterated with a spatiotemporal pattern that closely paralleled the directional elongation process (Fig. 8*B*). Thus, control of oriented cell spreading by focal adhesion positioning appeared to be spatially and temporally coupled to the pattern of Rac activation and associated lamellipodia extension.

Computer simulation of cell spreading on microarray of FN islands

To test whether spatial control of membrane process extension by ECM island location is sufficient to explain how the oriented cell spreading occurs that determines the subsequent cell migration direction, we created a computer simulation program to model the process of cell spreading on substrates with a discontinuous spatial distribution of ECM proteins. As described in Materials and Methods, this simulation program mimics the progressive events of cell adhesion to ECM islands, local extension of new membrane protrusions,

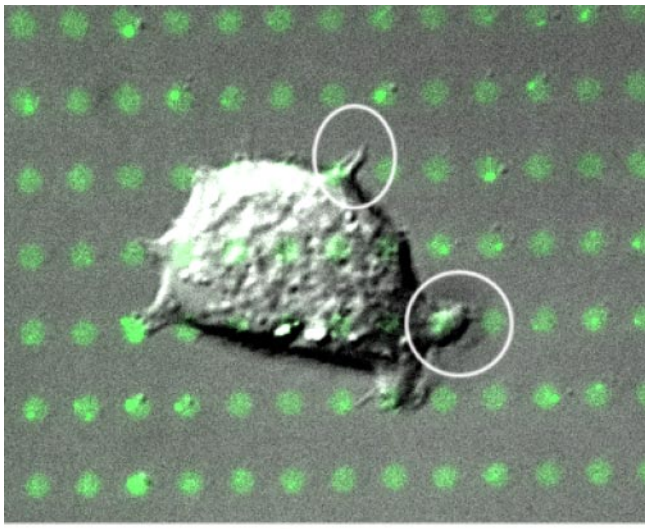

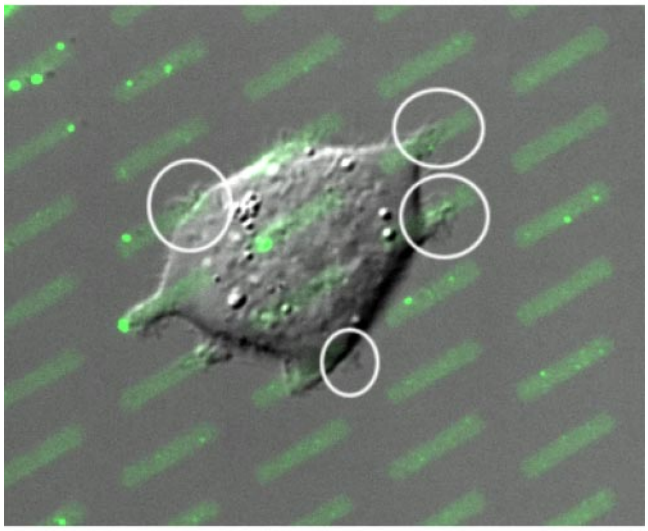

Figure 6. Overlays of Normarski and fluorescence microscopic images showing single cells spreading over multiple FN islands (green) on two different micropatterned substrates: 1C-1.5,3 and 8L-3,3st. Note that the cells preferentially extend new motile processes (white circles) from regions directly above where new adhesive contacts form with islands at the cell periphery. Images shown were acquired within 2 h after plating cells on micropatterns.

and formation of new adhesions and extension that we observed in our experimental studies (**Fig. 9*A***). The size distribution of the length of new membrane protrusions (Fig. 9*B*) was also based on experimental observations. The simulation results revealed that on the isotropic microarray of FN circles (1C-3,3), spreading cells develop heterogeneous shapes and random orientations (Fig. 9*C*, *E*). In contrast, on the anisotropic pattern of similar sized FN circles (1C-1.5,3), cells started from the very beginning of the spreading process to elongate preferentially in the *x* direction where the interisland spacing distances are smaller, and thus these cells gradually developed more elongated shapes compared to those on the isotropic circular islands (Fig. 9*D*, *E*). Interestingly, cell orientation reached optimal levels by early times (10 to 20 cycle iterations); whereas cells continued to elongate with repeated iterations (20 to 40 cycles) (Fig. 9*E*), much as we observed in studies with living cells (Fig. 3*A*, *B*).

When we simulated the effects of the six different FN island arrangements used in our experimental studies, we found that some patterns were more effective at aligning cells than the others, and cell elongation also proceeded at different paces on different patterns (Fig. 9*F*). Cell orientation was most dramatically influenced by altering the interisland spacing or the alignment of the islands, whereas changing island shape (*i.e.*, increasing the length of the islands) was relatively less effective. Importantly, when the simulation results describing the effects of all six island patterns on cell orientation were compared with experimental data, excellent correspondence between predictions and results were obtained (Fig. 9*G*). Thus, this simulation method could predict the effects of ECM island shape and position on both the spreading and orientation of cells that govern the direction in which they move.

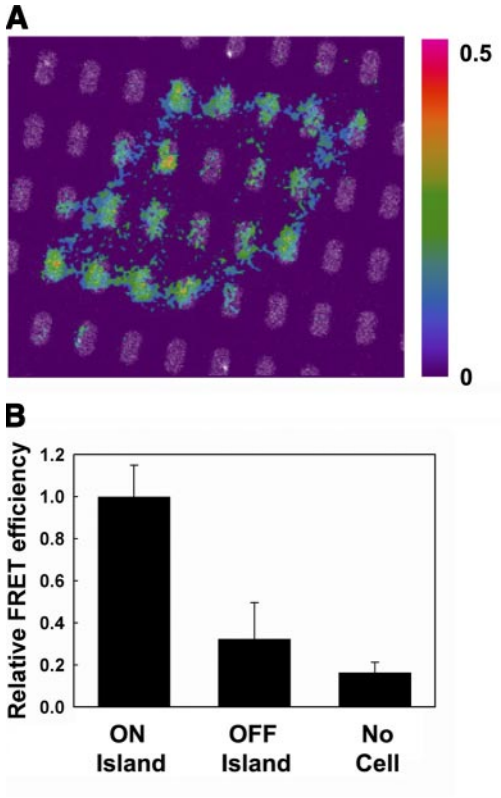

Figure 7. Rac-FRET analysis of Rac1 activity in cells adherent to micropatterned FN substrates. *A*) An overlay of fluorescence images showing Rac FRET efficiency, as indicated by the color bar (red is maximum), and the distribution of the FN islands (blue) underlying the same cell. Images shown were acquired within 2 h after plating cells on micropatterns. *B*) Comparison of FRET efficiencies measured in regions of cells directly above FN islands (ON Islands), over intervening noncoated regions of the substrate (OFF Islands), and in regions of the substrate over FN islands that are not covered by cells (No Cell).

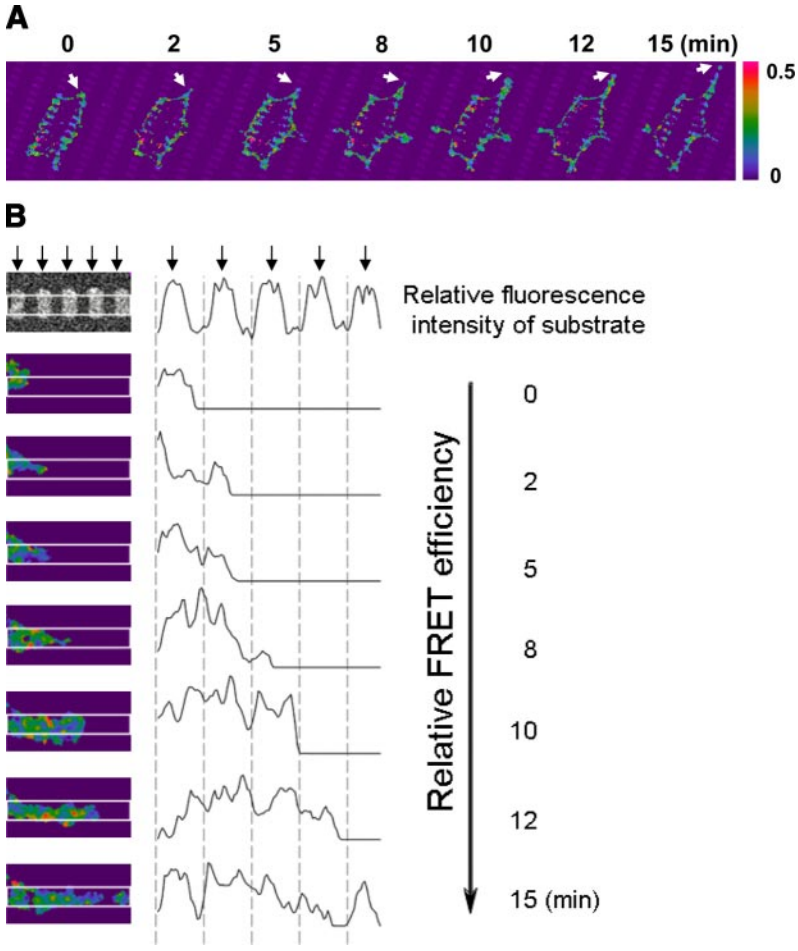

Figure 8. Time-lapse analysis of Rac-FRET efficiency reveals local control of Rac activation. *A*) Low-magnification view of Rac1 activity measured by FRET analysis within a whole cell spreading over multiple FN islands on a 3L-4.5,1 substrate during a period of 15 min. White arrowheads indicate increased Rac activity (FRET efficiency) concentrated in a dot-like pattern directly above FN islands at the top right portion of the cell, which is accompanied by cell extension in this direction over time. *B*) Higher-magnification view of 5 FN islands at the leading edge of the cell shown in *A*. Note that Rac activity is high above the most peripheral FN island the cell contacts at time 0 (first island at the left) and that it is elevated again when the cell touches the second island 2 min later; however, Rac FRET efficiency is low (blue) in the region of the cell membrane that overlies the intervening region of the substrate that is free of FN. This process reiterates as regions of low and high Rac activation are observed as the cell progressively extends new membrane and forms new FN contacts, respectively, as it spreads to the right over time. The black curved line indicates relative FRET efficiency quantitated over a line draw horizontally across these images; small arrows correspond to the position of each FN island; note the spatial correspondence between FN islands and higher Rac FRET efficiency. Images were recorded within 2 h after cell plating.

As a control, we modified the simulation program to permit membrane protrusions to be extended anywhere along the cell periphery (*i.e.*, rather than be restricted to regions in contact with the ECM islands) and found that cells spread with random orientation on the anisotropic patterns from the beginning of the spreading process (data not shown). Thus the spatial correspondence between the location of the ECM island and the position where new membrane processes protrude was critical to computer program's ability to successfully predict cell spreading and orientation behavior on these six different ECM substrates.

DISCUSSION

Control of directional cell motility is critical for embryogenesis, angiogenesis, inflammation, and tissue repair. Although most work in this field has assumed that oriented cell movement is controlled by gradients of soluble motility factors, recent results from a variety of experimental systems has shown that directional cell migration also can be regulated by local variations of ECM adhesion or mechanics (6, 8–10). For example, cells move up gradients of substrate stiffness and preferentially extend lamellipodia from their corners when physically constrained by being cultured on single cell-sized polygonal ECM islands (6, 9). The question remains: How are these physical environmental cues translated into changes in cell migration direction?

Past studies have suggested that focal adhesion position may govern this response based on the finding that focal adhesions often localize just behind the leading edge of migrating cells (25, 26, 33, 34) and that these cell anchoring complexes also contain multiple signaling molecules (*e.g.*, vinculin, Arp2/3) that are involved in the actin polymerization response that drives lamellipodia extension (35). Moreover, when individual cells are cultured on polygonal ECM islands, focal adhesions preferentially form in the same corner regions of these polygon-shaped cells where new lamellipodia extend (8, 9). However, these are only correlations: a causal role for focal adhesion position in control of directional cell movement has never been demonstrated.

Here we addressed this challenge directly by using a microfabrication technique to present ECM molecules in a predefined spatial distribution at the micrometer scale in order to exert spatial control over focal adhesion positioning in living cells. Using this approach, we found that lamellipodia preferentially form in close proximity to nascent focal adhesions that form where cells form new contacts to ECM islands along the cell periphery. Moreover, by changing the shape, size, and spacing of the islands, we could promote formation of focal adhesions and associated lamellipodia as well as

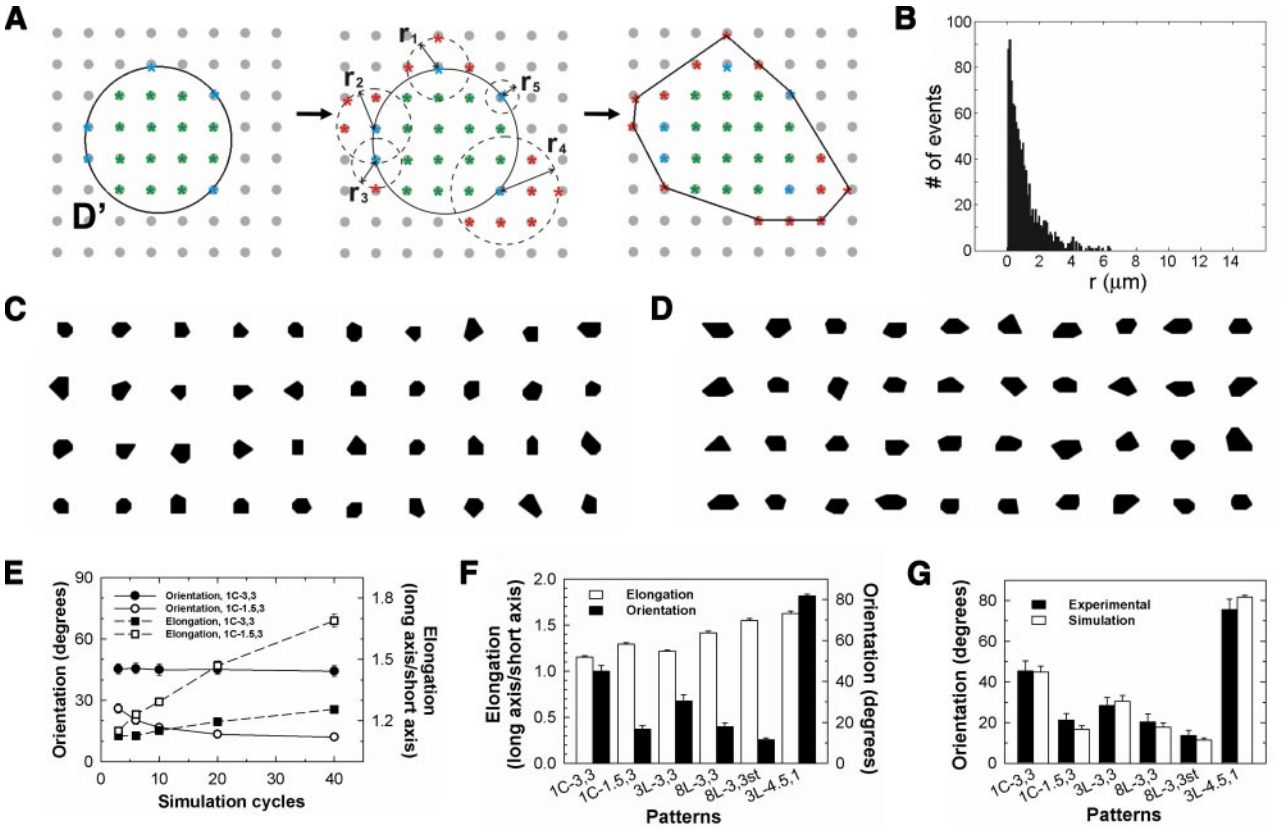

Figure 9. Computer simulation of cell spreading on FN microarrays. *A*) Schematic illustration of the simulated cell spreading process. Solid circle indicates contact area of diameter D' between the simulated cell and the culture substrate; smaller stippled circles indicate range of extension of individual membrane protrusions with radius r that extend from peripheral contacts with underlying FN islands. *B*) Histogram of the distribution of lengths (radii) of cellular protrusions used in the simulation that is based on experimental observations. *C*) Simulated cell shapes obtained after 20 cycles of spreading on the 1C-3,3 substrate (100 cells were generated at each time point; 40 representative final cell shapes are shown here). *D*) Similar results obtained with simulated cells on the 1C-1.5,3 substrate. *E*) Graph showing the effects of simulation cycle number on cell elongation and orientation on the 1C-3,3 and 1C-1.5,3 substrates. *F*) Comparison of the simulation predictions generated with 40 cycles of cell spreading for the effects of all six types of FN microarrays on cell elongation and orientation. *G*) A similar comparison of the simulation predictions (40 cycles) with experimental results (measured 2 h after plating) describing the effects of the different FN subtrates on cell orientation.

associated cell elongation in an oriented manner. Most importantly, this oriented response also governed the direction in which the cells moved when subsequently stimulated by soluble motility factors. Thus, physical cues from the ECM appear to control directional cell motility by governing where cells will form new focal adhesions.

These experimental findings were supported by the development of a computational simulation that predicted the effects of all six different ECM micropatterns with great precision. In the simulation, the cell diameter D and the initial diameter of the cell-substrate contact area D' were both set as 15 μm. In reality, D' is often smaller than D; however, when we reduced the value of D' to $D/3$ or $D/2$, the aforementioned trends observed with the simulation results remained unchanged (not shown). The radius r of radial extension in the simulation was computer generated each time an extension was made following a preset size distribution rule for r in our simulation. Although it was technically possible to incorporate any size distribution rule for r into the program, we assumed in our simulation that large extensions decreased exponentially with r based on observations with living cells in our studies. This makes sense given that the formation of membrane protrusions requires energy as well as the ability to concentrate multiple molecules involved in the membrane protrusion machinery within a small region of the cell surface; thus, small protrusions would be expected to be more likely and more easy to form than large ones.

In the computational model, we also assumed that each intersection between the cell periphery and an adhesive island had an equal capability to form a membrane protrusion. This assumption was derived from our experimental observation that, regardless of cell shape, membrane protrusions formed stochastically in regions of FN islands distributed all along the cell periphery with no perceptible directional bias (Fig. 4), and membrane protrusion has been similarly been shown to be a random, nonoriented process in cells cultured on standard tissue culture substrates (*i.e.*, coated with a homogenous layer of ECM components) (36). Thus, this assumption seems reasonable, especially given the ability of our model to predict initial spreading and orientation behavior with great precision.

The spreading process in the simulation is a probability-driven process, and the only constraint is spatial restriction to protrusion formation in regions near focal adhesions. In the absence of this single constraint, cells spread with random orientation even on the anisotropic micropatterns. This is important because our experimental findings confirmed that membrane protrusive activity is activated by cell adhesion to ECM and spatially constrained to regions near newly formed focal adhesions. Furthermore, cells started to extend anisotropically from the very beginning of the spreading process on the anisotropic micropatterns. Taken together with our past observations that increasing the distance between adjacent ECM islands greatly decreases the likelihood of a cell spanning two islands (28), these results suggest that the delay in spreading we observed here on ECM islands compared to unpatterned substrates is due to the large nonadhesive regions that separate the islands. Essentially, the cells have to extend longer lamellipodia over much larger distances than on unpatterned substrates to form new matrix contacts. But the simulation could also predict that ECM islands of different shape (*e.g.*, 1 μm circles *vs.* 8 μm lines) will promote different degrees of elongation. This result may be due to the fact that longer lines produce continuous sites for new adhesions in the same direction as the cell progressively spreads (and D' increases) and extends new protrusions.

Focal adhesion formation has been shown to be sensitive to the level of mechanical forces that cells generate and exert on their ECM adhesions. Focal adhesion assembly increases with higher levels of cytoskeletal tension controlled by the Rho-ROCK pathway, whereas tension dissipation leads to focal adhesion disassembly (27). The adhesive islands studied in the present study were microprinted with the same FN coating concentration, and they all were similarly rigid. However, they differed in their ability to resist and support cell tractional forces exerted in different directions because of variations of their size, shape, and position. For example, a linear adhesive island aligned with the long axis of a cell can resist higher traction forces in that direction (due to exposure of more ECM contact area along the applied tension field lines) and hence promote linear assembly of focal adhesions and greater actin stress fiber formation and alignment in this direction relative to a circular island. Thus, the shape and orientation of the focal adhesions that formed closely matched that of the micropatterned FN islands. This is also analogous to what happens when cells are cultured on ECM substrates that exhibit gradients of mechanical stiffness where larger focal adhesions form on the pole of the cell that contacts the more rigid ECM that can better resist cell tensional forces (6).

Cells continually realign their internal cytoskeletal filaments (*e.g.*, stress fibers) along the applied tension lines that are dictated by their unique pattern of fixed adhesions. As we demonstrated experimentally, if focal adhesions are evenly distributed and isotropic in form, the cell and cytoskeleton orient randomly relative to the substrate. However, if these evenly distributed adhesions are all linear in form and oriented in the same direction, the structural bias of the focal adhesions also will generate an oriented tension field when the cell pulls against them. This will promote realignment of the actin cytoskeleton until the stress fibers orient along this same axis, and all stresses will be brought into balance. Similarly, because the likelihood that cells will form new adhesive contact increases as the spacing between neighboring islands decreases, cells will preferentially spread in the direction that crosses the minimum interisland spacing distance on each substrate. In fact, interisland spacing had a dramatic effect on cell orientation and directional migration compared to the shape and size of the focal adhesions. Moreover, when these cells exert tractional forces on multiple fixed contacts oriented in a single direction, the actin cytoskeleton will again progressively reorient itself along this same axis in order to minimize tensional stresses. A related response may occur during durotaxis because cells will form stronger focal adhesions and greater mechanical resistance sites at one end of the cell and thereby create a similar tension axis (in this case, extending from regions of low to high ECM rigidity) that again predicts the direction of cell spreading, actin alignment, and movement.

Thus, our results suggest that directional cell movement may be controlled through a mechanochemical mechanism that involves both local and global physical interactions between the cell and the ECM substrate. Importantly, however, the chemical composition of focal adhesions also varies across the bottom surface of the cell. For example, we found that while vinculin appeared relatively evenly distributed in focal adhesions throughout the basal cell surface, other molecules that are critical for motility signaling, such as activated Rac, only appeared along with vinculin in focal adhesions located directly above ECM islands along the cell periphery. Our real-time imaging studies confirmed that these represent the most newly formed (nascent) focal adhesions, or focal complexes, that have previously shown to be enriched for these signaling molecules (23). More importantly, using Rac-FRET analysis we could demonstrate directly that Rac becomes activated locally within these nascent focal adhesions within minutes after ECM binding and that it triggers lamellipodia extension from adjacent sites. This finding might be mediated by phosphorylation of the focal adhesion protein paxillin, which has been shown to activate Rac and thereby up-regulate focal adhesion turnover and protrusion formation by recruiting the RacGEF complex, GIT1-PIX-PAK to new adhesion sites (33, 34). In separate studies, we also showed that the initial direction of lamellipodia extension governs the orientation in which the cell will subsequently elongate, and the direction in which it will move when stimulated by soluble chemokines. Moreover, using computer simulation, this spatial coupling between focal adhesion formation and new membrane protrusion was shown to be sufficient to predict the cell elongation and orientation results we obtained in our experimental studies. Taken together, these results show that physical cues from the ECM govern

the direction in which the cell will move by directing where the cell will form new focal adhesions, which, in turn, determines where motility signal responses will be activated inside the cell. FJ

These studies were supported by U.S. National Institutes of Health grant CA45548 and National Science Foundation grant DMR-0213805 in support of the Materials Research Science and Engineering Center of Harvard University.

REFERENCES

1. Ridley, A. J., Schwartz, M. A., Burridge, K., Firtel, R. A., Ginsberg, M. H., Borisy, G., Parsons, J. T., and Horwitz, A. R. (2003) Cell migration: integrating signals from front to back. *Science* **302,** 1704–1709
2. Ueda, M., Sako, Y., Tanaka, T., Devreotes, P., and Yanagida, T. (2001) Single-molecule analysis of chemotactic signaling in Dictyostelium cells. *Science* **294,** 864–867
3. Van Haastert, P. J. M., and Devreotes, P. N. (2004) Chemotaxis: signalling the way forward. *Nat. Rev. Mol. Cell. Biol.* **5,** 626–634
4. Xiao, Z., Zhang, N., Murphy, D. B., and Devreotes, P. N. (1997) Dynamic distribution of chemoattractant receptors in living cells during chemotaxis and persistent stimulation. *J. Cell Biol.* **139,** 365–374
5. Discher, D. E., Janmey, P., and Wang, Y. L. (2005) Tissue cells feel and respond to the stiffness of their substrate. *Science* **310,** 1139–1143
6. Lo, C. M., Wang, H. B., Dembo, M., and Wang, Y. L. (2000) Cell movement is guided by the rigidity of the substrate. *Biophys. J.* **79,** 144–152
7. Peyton, S. R., and Putnam, A. J. (2005) Extracellular matrix rigidity governs smooth muscle cell motility in a biphasic fashion. *J. Cell. Physiol.* **204,** 198–209
8. Brock, A., Chang, E., Ho, C. C., LeDuc, P., Jiang, X. Y., Whitesides, G. M., and Ingber, D. E. (2003) Geometric determinants of directional cell motility revealed using microcontact printing. *Langmuir* **19,** 1611–1617
9. Parker, K. K., Brock, A. L., Brangwynne, C., Mannix, R. J., Wang, N., Ostuni, E., Geisse, N. A., Adams, J. C., Whitesides, G. M., and Ingber, D. E. (2002) Directional control of lamellipodia extension by constraining cell shape and orienting cell tractional forces. *FASEB J.* **16,** 1194–1204
10. Jiang, X. Y., Bruzewicz, D. A., Wong, A. P., Piel, M., and Whitesides, G. M. (2005) Directing cell migration with asymmetric micropatterns. *Proc. Natl. Acad. Sci.* **102,** 975–978
11. Nakatsuji, N., and Johnson, K. E. (1984) Experimental manipulation of a contact guidance system in amphibian gastrulation by mechanical tension. *Nature* **307,** 453–455
12. Folkman, J., Watson, K., Ingber, D., and Hanahan, D. (1989) Induction of angiogenesis during the transition from hyperplasia to neoplasia. *Nature* **339,** 58–61
13. Geiger, B., Bershadsky, A., Pankov, R., and Yamada, K. M. (2001) Transmembrane extracellular matrix-cytoskeleton crosstalk. *Nat. Rev. Mol. Cell. Biol.* **2,** 793–805
14. Clark, E. A., King, W. G., Brugge, J. S., Symons, M., and Hynes, R. O. (1998) Integrin-mediated signals regulated by members of the Rho family of GTPases. *J. Cell Biol.* **142,** 573–586
15. Del Pozo, M. A., Price, L. S., Alderson, N. B., Ren, X. D., and Schwartz, M. A. (2000) Adhesion to the extracellular matrix regulates the coupling of the small GTPase Rac to its effector PAK. *EMBO J.* **19,** 2008–2014
16. Price, L. S., Leng, J., Schwartz, M. A., and Bokoch, G. M. (1998) Activation of Rac and Cdc42 by integrins mediates cell spreading. *Mol. Biol. Cell* **9,** 1863–1871
17. Higgs, H. N., and Pollard, T. D. (2001) Regulation of actin filament network formation through Arp2/3 complex: Activation by a diverse array of proteins. *Annu. Rev. Biochem.* **70,** 649–676
18. Machesky, L. M., Atkinson, S. J., Ampe, C., Vandekerckhove, J., and Pollard, T. D. (1994) Purification of a cortical complex containing 2 unconventional actins from acanthamoeba by affinity-chromatography on profilin-agarose. *J. Cell Biol.* **127,** 107–115
19. Mullins, R. D., Heuser, J. A., and Pollard, T. D. (1998) The interaction of Arp2/3 complex with actin: nucleation, high affinity pointed end capping, and formation of branching networks of filaments. *Proc. Natl. Acad. Sci.* **95,** 6181–6186
20. Svitkina, T. M., and Borisy, G. G. (1999) Arp2/3 complex and actin depolymerizing factor cofilin in dendritic organization and treadmilling of actin filament array in lamellipodia. *J. Cell Biol.* **145,** 1009–1026
21. Nobes, C. D., and Hall, A. (1995) Rho, Rac, and Cdc42 Gtpases regulate the assembly of multimolecular focal complexes associated with actin stress fibers, lamellipodia, and filopodia. *Cell* **81,** 53–62
22. Ridley, A. J., Paterson, H. F., Johnston, C. L., Diekmann, D., and Hall, A. (1992) The small Gtp-binding protein Rac regulates growth-factor induced membrane ruffling. *Cell* **70,** 401–410
23. DeMali, K. A., Barlow, C. A., and Burridge, K. (2002) Recruitment of the Arp2/3 complex to vinculin: coupling membrane protrusion to matrix adhesion. *J. Cell Biol.* **159,** 881–891
24. Goldmann, W. H., and Ingber, D. E. (2002) Intact vinculin protein is required for control of cell shape, cell mechanics, and rac-dependent lamellipodia formation. *Biochem. Biophys. Res. Commun.* **290,** 749–755
25. Beningo, K. A., Dembo, M., Kaverina, I., Small, J. V., and Wang, Y.-l. (2001) Nascent focal adhesions are responsible for the generation of strong propulsive forces in migrating fibroblasts. *J. Cell Biol.* **153,** 881–888
26. Pelham, R. J., Jr., and Wang, Y.-l. (1997) Cell locomotion and focal adhesions are regulated by substrate flexibility. *Proc. Natl. Acad. Sci.* **94,** 13661–13665
27. Riveline, D., Zamir, E., Balaban, N. Q., Schwarz, U. S., Ishizaki, T., Narumiya, S., Kam, Z., Geiger, B., and Bershadsky, A. D. (2001) Focal contacts as mechanosensors: externally applied local mechanical force induces growth of focal contacts by an mDia1-dependent and ROCK-independent mechanism. *J. Cell Biol.* **153,** 1175–1186
28. Chen, C. S., Alonso, J. L., Ostuni, E., Whitesides, G. M., and Ingber, D. E. (2003) Cell shape provides global control of focal adhesion assembly. *Biochem. Biophys. Res. Commun.* **307,** 355–361
29. Tan, J. L., Liu, W., Nelson, C. M., Raghavan, S., and Chen, C. S. (2004) Simple approach to micropattern cells on common culture substrates by tuning substrate wettability. *Tissue Eng.* **10,** 865–872
30. Itoh, R. E., Kurokawa, K., Ohba, Y., Yoshizaki, H., Mochizuki, N., and Matsuda, M. (2002) Activation of Rac and Cdc42 video imaged by fluorescent resonance energy transfer-based single-molecule probes in the membrane of living cells. *Mol. Cell. Biol.* **22,** 6582–6591
31. Roberts, C., Mrksich, M., Martichonok, V., Ingber, D. E., and Whitesides, G. M. (1998) Using mixed self assembled monolayers presenting GRGD and EG3OH groups to characterize long-term attachment of bovine capillary endothelial cells to surfaces. *J. Am. Chem. Soc.* **120,** 6548–6555
32. Mooney, D. J., Langer, R., and Ingber, D. E. (1995) Cytoskeletal filament assembly and the control of cell spreading and function by extracellular matrix. *J. Cell Sci.* **108,** 2311–2320
33. Nayal, A., Webb, D. J., Brown, C. M., Schaefer, E. M., Vicente-Manzanares, M., and Horwitz, A. R. (2006) Paxillin phosphorylation at Ser273 localizes a GIT1-PIX-PAK complex and regulates adhesion and protrusion dynamics. *J. Cell Biol.* **173,** 587–589
34. Webb, D. J., Donais, K., Whitmore, L. A., Thomas, S. M., Turner, C. E., Parsons, J. T., and Horwitz, A. F. (2004) FAK-Src signalling through paxillin, ERK and MLCK regulates adhesion disassembly. *Nat. Cell Biol.* **6,** 154–161
35. DeMali, K. A., and Burridge, K. (2003) Coupling membrane protrusion and cell adhesion. *J. Cell Sci.* **116,** 2389–2397
36. Dubin-Thaler, B. J., Giannone, G., Dobereiner, H. G., and Sheetz, M. P. (2004) Nanometer analysis of cell spreading on matrix-coated surfaces reveals two distinct cell states and STEPs. *Biophys. J.* **86,** 1794–1806
37. Condeelis, J. (1993) Life at the leading-edge - the formation of cell protrusions. *Annu. Rev. Cell Biol.* **9,** 411–444
38. Chen, C. S., Mrksich, M., Huang, S., Whitesides, G. M., and Ingber, D. E. (1997) Geometric control of cell life and death. *Science* **276,** 1425–1428

Received for publication June 6, 2007.
Accepted for publication December 6, 2007.